SCIENCE CHINA
Chemistry

• ARTICLES •

March 2014 Vol.57 No.3: 371–378
doi: 10.1007/s11426-013-4926-5

p-Sulfonatocalix[4]arene-induced amphiphilic aggregation of fluorocarbon surfactant

CAO Yu, WANG YiXuan, GUO DongSheng & LIU Yu*

State Key Laboratory of Elemento-Organic Chemistry; Department of Chemistry, Nankai University, Tianjin 300071, China

Received June 3, 2013; accepted June 24, 2013; published online August 12, 2013

Sulfonatocalix[4]arene lowers the critical aggregation concentration of fluorocarbon surfactant pronouncedly by a factor of ca. 100 to form binary amphiphilic aggregates on the basis of host-guest complexation, which was identified by ^{1}H NMR spectroscopy, fluorescence spectroscopy, optical transmittance spectroscopy, dynamic laser scattering, high-resolution transmission electron microscopy, scanning electron microscopy, and surface tension experiments. Moreover, the resulting aggregates can respond to external stimuli, including temperature and inclusion of competitor guest. Therefore, the present system may have potential applications in drug delivery systems.

calixarene-induced aggregates, fluorocarbon surfactant, supra-amphiphile, multi-stimuli responses

1 Introduction

In recent years, researches on supra-amphiphile have become quite fascinating owing to its simplicity, versatility, and especially reversibility, which endow its typical applications in various fields of chemistry, biology, and materials science [1–6]. Macrocyclic compounds [7–11], such as crown ethers, cyclodextrins, calixarenes, and cucurbiturils, have exhibited great advantages in building supramolecular architectures [12, 13]. Among them, calixarenes [14], composed of phenolic units linked by methylene bridges, have been frequently employed in building self-assembled nanoscaled micellar and vesicular aggregation on the basis of their intrinsic cone shape and relatively rigid framework [15]. However, construction of calixarene-based supra-amphiphile is still a challenging topic up to now.

p-Sulfonatocalix[*n*]arenes (SCnAs), which are demonstrated to promise biological, pharmaceutical, analytical and crystal-engineering applications, generate versatile inclusion/complexation properties for kinds of guest molecules [16, 17]. We and others recently have found that SCnAs possess the capability of inducing the aggregation of cationic surfactants to form supramolecular vesicles, micelles, and other amphiphilic assemblies [18–21]. Owing to the host-guest complexation, calixarenes can decrease the critical aggregation concentration (CAC) of free amphiphilic molecules to obtain higher-order assemblies. Calixarene-induced aggregates (CIAs) have potential applications in drug delivery, gene therapy and biomembrane modeling systems [22, 23], as these nanostructrues are easy to be tuned and also response to several external stimuli such as temperature, pH, voltage, redox and light [24–28].

On the other hand, fluorocarbon surfactants, substituted H atoms in traditional hydrocarbon surfactants with F atoms, are a particular class of functionalized amphiphilic molecules exhibiting surface activity in both aqueous and organic solutions [29]. Moreover, they are quite stable in heating, acid, base, as well as oxidizing and reducing solutions [30]. These unique features endow them irreplaceable applications in several fields, such as paints, waxes, pharmaceuticals, firefighting foams, plane hydraulic fluids, and coatings for clothing fabrics [31, 32].

Our particular interest herein is to fabricate CIAs through

*Corresponding author (email: yuliu@nankai.edu.cn)

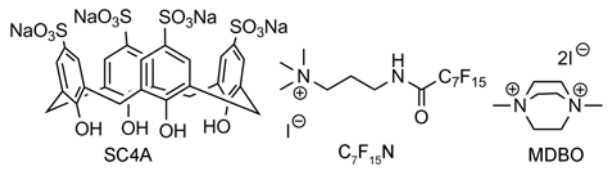

Scheme 1 Structural illustration of SC4A, $C_7F_{15}N$, and competitor guest 1,4-dimethyldiazabicyclo[2.2.2]octane (MDBO).

host-guest complexation of SC4A with fluorocarbon surfactant $C_7F_{15}CONH(CH_2)_3NCH_3I$ ($C_7F_{15}N$) (Scheme 1). Combining advantages of calixarenes and fluorocarbon surfactants, we expect a novel smart material showing feasible applications in drug delivery and controlled release systems.

2 Experimental

Fluorocarbon surfactant $C_7F_{15}N$ and 4-phenolsulfonic sodium were commercially available from Beijing FLUOBON Surfactant Institute and Acros, respectively. They were used without further purification. SC4A [33–35] and MDBO [36] were synthesized and purified according to the procedures reported previously.

^{1}H NMR spectra were recorded on a Bruker AV400 spectrometer in D_2O at 25 °C.

Steady-state fluorescence spectra were recorded in a conventional quartz cell (light path 10 mm) on a Varian Cary Eclipse equipped with a Varian Cary single-cell Peltier accessory to control the temperature (λ_{ex} = 335.0 nm, bandwidth (ex) 10 nm, bandwidth (em) 2.5 nm).

The optical transmittance of the aqueous solution was measured in a quartz cell (light path 10 mm) on a Shimadzu UV-3600 spectrophotometer equipped with a PTC-348WI temperature controller.

The static surface tension in aqueous solution was measured by using a QBZY full-automatic surface tensiometer by the method of platinum plate at 25 °C.

The sample solution for dynamic laser scattering (DLS) measurements was prepared by filtering the solution through a 450 nm Millipore filter into a clean scintillation vial. The samples were examined on a laser light scattering spectrometer (BI-200SM) equipped with a digital correlator (Turbo Corr.) at 532 nm at a scattering angle of 90°. The concentrations of SC4A and $C_7F_{15}N$ were 0.04 and 0.15 mM, respectively.

High-resolution transmission electron microscopy (TEM) images were recorded on a Tecnai 20 high resolution transmission electron microscope operating at an accelerating voltage of 200 keV. The sample for TEM measurements was prepared by dropping the solution onto a copper grid. The grid was then air-dried. Scanning electron microscopy (SEM) images were recorded on a Hitachi S-3500N scanning electron microscope. The sample for SEM measurements was prepared by dropping the solution onto a coverslip, followed by evaporating the liquid in air. The concentrations of SC4A and $C_7F_{15}N$ were 0.04 and 0.15 mM, respectively.

3 Results and discussion

A supramolecular amphiphilic assembly was fabricated on the basis of host-guest complexation of SC4A with $C_7F_{15}N$. ^{1}H NMR measurements were performed to determine the host-guest inclusion phenomenon. As shown in Figure 1, the proton signal of quaternary ammonium undergoes upfield chemical shift and the $\Delta\delta$ ($\Delta\delta = \delta_{complex} - \delta_{free}$) is –2.01. This indicates that the cationic head group of $C_7F_{15}N$ penetrates into the calixarene cavity, as protons of the quaternary ammonium are affected by the ring current effect of the aromatic nuclei of calixarene. This notable chemical shift confirms the inclusion interaction between SC4A and $C_7F_{15}N$.

Free $C_7F_{15}N$ generates amphiphilic assembly spontaneously owing to its hydrophilic quaternary ammonium head group and hydrophobic fluorocarbon long chain. Its CAC was determined by monitoring the relative fluorescence intensity of pyrene probe molecules. Kalyanasundaram and Thomas [37] have demonstrated that vibronic band intensities in pyrene monomer fluorescence can be used as a convenient probe to accurately measure CAC values. The dependence of relative fluorescence intensity of pyrene (III/I ratio) on the concentration of $C_7F_{15}N$ increases gradually, showing a sigmoid curvature as fluorocarbon surfactant provides hydrophobic domain above CAC. As can be seen from Figure 2, the CMC is estimated to be 6.0 mM.

The complexation of SC4A with $C_7F_{15}N$ would generate large-size aggregates affecting the optical transmittance of solutions. The CAC value of $C_7F_{15}N$ in the presence of SC4A was then determined by monitoring the dependence of the transmittance at 450 nm on the concentration of $C_7F_{15}N$ [38–40]. In the absence of SC4A, the transmittance of $C_7F_{15}N$ solution at 450 nm displays no appreciable change as the concentration of $C_7F_{15}N$ increases from 0.01 mM to 0.20 mM (Figure 3(a)). In the presence of SC4A, the transmittance of solution decreases gradually as the concentration of $C_7F_{15}N$ increases, which results from an amphiphilic assembly of large size (Figure 3(b–d)). According to the plot of transmittance at 450 nm versus concentration of $C_7F_{15}N$, two lines can be obtained and the intersection point represents the calixarene-induced CAC value. As shown in Figure 3(b–d) insets, the CAC of SC4A+$C_7F_{15}N$ complexation is evaluated to be 0.07 mM at 0.02 mM SC4A, 0.08 mM at 0.05 mM SC4A, and 0.10 mM at 0.08 mM SC4A, respectively. Excitingly, the CAC value of $C_7F_{15}N$ decreases pronouncedly by a factor of ca. 100 owing to the complexation of SC4A. In a control experiment, SC4A has no tendency to self-aggregate in aqueous solution [41].

Surface tension measurements were further conducted to

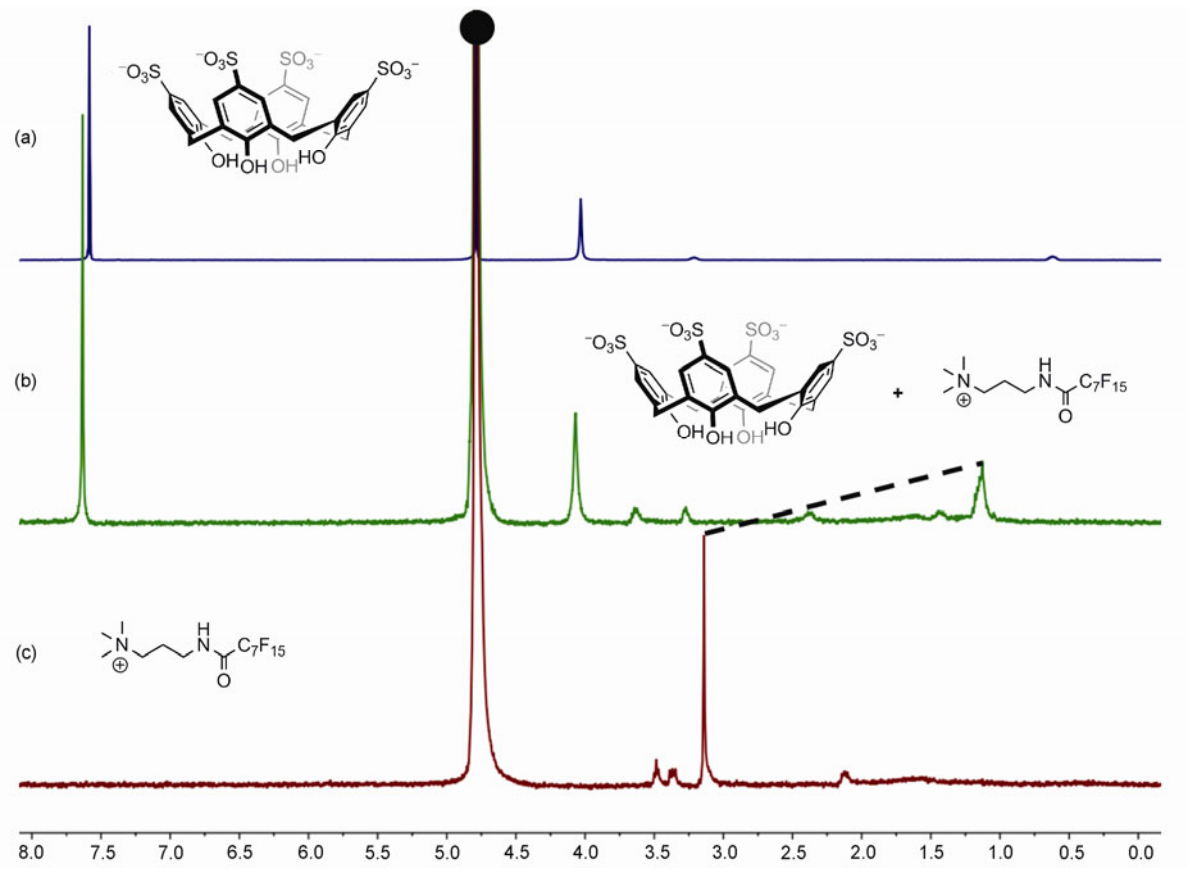

Figure 1 ^{1}H NMR spectra of SC4A (a), SC4A+$C_7F_{15}N$ complex (b) and $C_7F_{15}N$ (c) in D_2O (1.0 mM). The solvent (H_2O) is denoted as symbol ●.

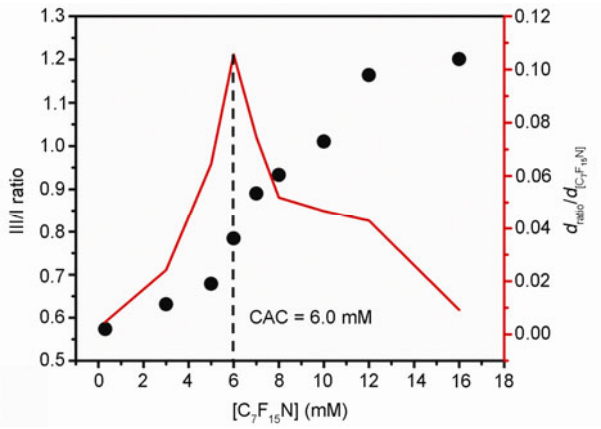

Figure 2 Dependence of III/I ratio on the concentration of $C_7F_{15}N$ (25 °C). [pyrene] = 0.001 mM. λ_{ex} = 335 nm. I and III represent fluorescence intensity of pyrene at 372 nm and 383 nm, respectively.

detect the distinguishable amphiphilic aggregation between SC4A and $C_7F_{15}N$ (Figure 4). In the presence of 0.04 mM SC4A, the surface tension of the solution decreases continuously with adding $C_7F_{15}N$ until a minimum is reached, and after that the value is tend toward an equilibrium state, indicating that binary complex starts to aggregate in aqueous solution. The CAC of $C_7F_{15}N$ in the presence of 0.04 mM SC4A determined by the surface tension measurements is 0.06 mM, agreeing well with the result from optical transmittance spectra. Moreover, the result displays that the SC4A+$C_7F_{15}N$ aggregates are amphiphilic due to the remarkable decline of surface tension.

In experiments above, SC4A can indeed decrease the CAC value of $C_7F_{15}N$ remarkably. However, it is still prerequisite to determine the optimal molar fraction between SC4A and $C_7F_{15}N$ to construct a robust amphiphilic assembly. Figure 5 shows the optical transmittance spectra and the plot of transmittance at 450 nm as a function of the concentration of SC4A with a fixed $C_7F_{15}N$ concentration at 0.15 mM. The transmittance at 450 nm undergoes a rapid decrease and then a gradual increase to reach a quasi-plateau upon addition of SC4A. In the left-hand portion of the curve, a higher-order complex is formed by SC4A and $C_7F_{15}N$ with a tendency toward amphiphilic aggregation, whereas in the right-hand portion, the formed complex disassembles upon addition of excess SC4A to a simple inclusion complex. The minimum transmittance point reaches at 0.04 mM SC4A, and the inflection appears at a SC4A/$C_7F_{15}N$ molar ratio of 4:15, representing the best molar fraction of SC4A/$C_7F_{15}N$ for the amphiphilic assembly. The solution of SC4A+$C_7F_{15}N$ system exhibits clear Tyndall effect (Figure 5 inset), which reveals the existence of abundant nanoparticles.

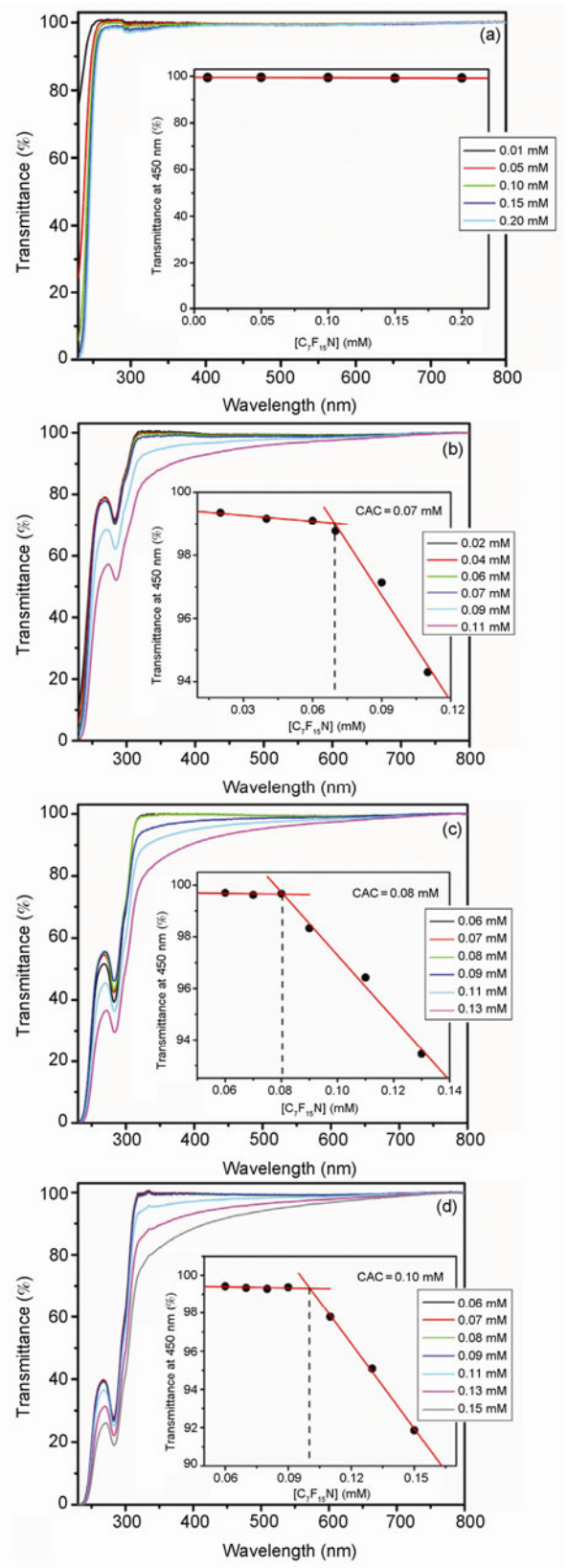

Figure 3 Optical transmittance of aqueous solutions of $C_7F_{15}N$ at different concentrations in the absence (a) and presence of SC4A: (b) 0.02 mM, (c) 0.05 mM, (d) 0.08 mM at 25 °C. Insets: dependence of the transmittance at 450 nm on $C_7F_{15}N$ concentration in the absence (a) and presence of SC4A: (b) 0.02 mM, (c) 0.05 mM, and (d) 0.08 mM.

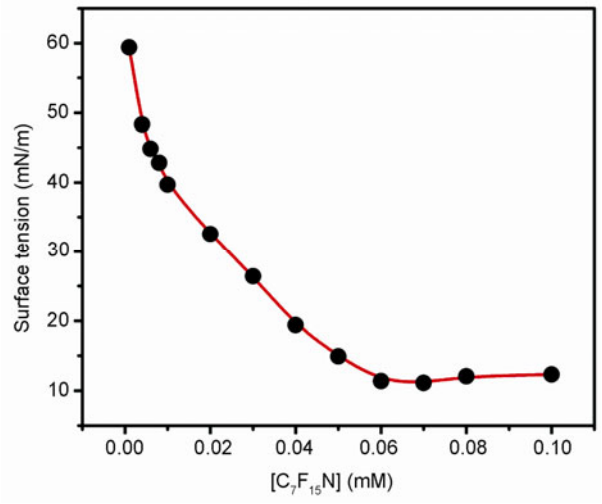

Figure 4 Surface tension data of aqueous solutions of $C_7F_{15}N$ at different concentrations in the presence of 0.04 mM SC4A at 25 °C.

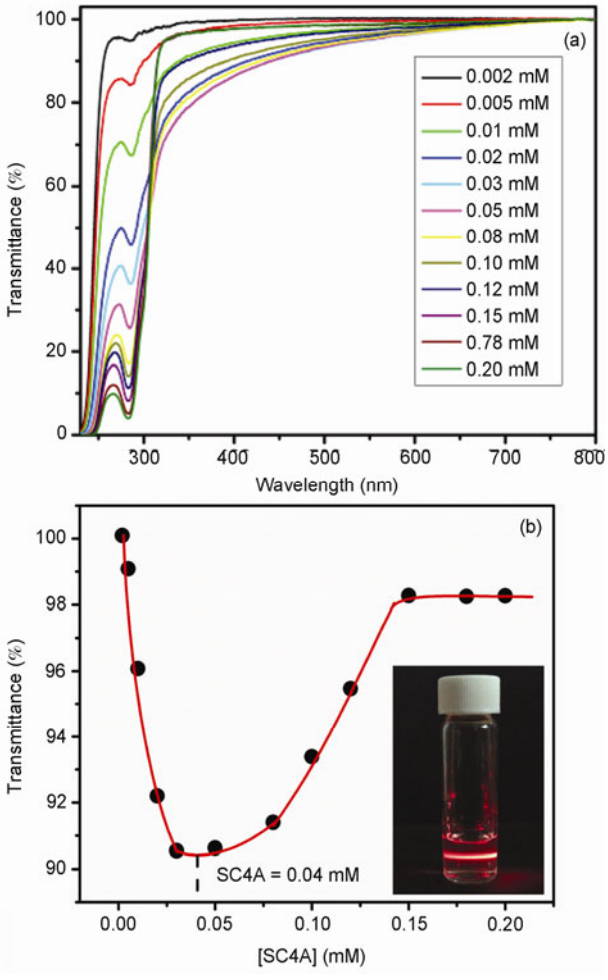

Figure 5 (a) Optical transmittance of aqueous solutions of SC4A at different concentrations in the presence of 0.15 mM $C_7F_{15}N$ at 25 °C; (b) dependence of the transmittance at 450 nm on SC4A concentration in the presence of 0.15 mM $C_7F_{15}N$. Inset: tyndall effect of SC4A+$C_7F_{15}N$ system, [SC4A] = 0.04 mM, [$C_7F_{15}N$] = 0.15 mM.

Control experiments show that replacing SC4A by its building unit 4-phenolsulfonic sodium cannot decrease the transmittance at 450 nm of the system (Figure 6), which indicates that the aggregation of $C_7F_{15}N$ results mainly from the host-guest complexation of SC4A. Electrostatic interactions between the negative sulfonate groups and positive quaternary ammonium groups reinforce the complex stability. Furthermore, the descending transmittance at 450 nm in a normal saline solution reveals that SC4A and $C_7F_{15}N$ can still form amphiphilic aggregates in high ionic strength medium.

Stability of the SC4A+$C_7F_{15}N$ (4:15) aggregates was measured by monitoring the dependence of the transmittance at 450 nm on the time variation. As can be seen from Figure 7, the transmittance at 450 nm of the solution undergoes a drop before 100 min showing the gradual formation of the supermolecular nanoscaled aggregates, and the system has tendency to reach the stable state after 100 min.

DLS, TEM and SEM were employed to identify the size and morphology of the amphiphilic SC4A+$C_7F_{15}N$ (4:15) aggregates. In DLS measurements, free $C_7F_{15}N$ does not exhibit a size distribution under the same conditions, indicating that no aggregates have been formed (Figure 8(a)). However, amphiphilic aggregates generated by the complex exhibit a narrow size distribution, giving an average diameter of 392 nm at a scattering angle of 90° (Figure 8(b)), which is larger than the aggregates (194 nm) formed by SC4A and hydrocarbon surfactant myristoylcholine possessing similar structure and CMC [23]. This is because larger volume of fluorine atoms and stronger hydrophobicity of fluorocarbon chains led by the high electronegativity of fluorine atoms result in the fluorocarbon surfactant $C_7F_{15}N$ occupying greater hydrophobic area inside the membranes than hydrocarbon surfactant myristoylcholine. Therefore, the curvature radius of the SC4A+$C_7F_{15}N$ aggregates is larger than that of the SC4A+myristoylcholine aggregates.

SEM images (Figure 9(a, b)) show the spherical morphology with a diameter ranging from 200 to 500 nm, in nice agreement with the DLS result (Figure 8(b)). Such spheres are also found in TEM images (Figure 9(c, d)).

The SC4A+$C_7F_{15}N$ aggregate has the capability of responding to external stimuli, such as temperature and host-guest inclusion [42, 43]. Temperature is a useful signal with easy and safe medical applications in comparison with the rest external stimuli [44]. The SC4A+$C_7F_{15}N$ aggregate

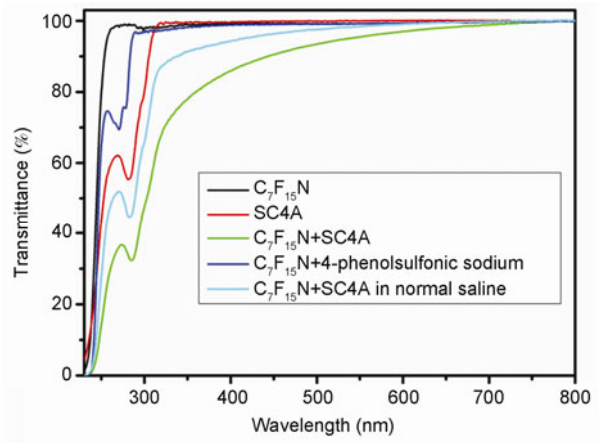

Figure 6 Optical transmittance of $C_7F_{15}N$, SC4A, $C_7F_{15}N$+SC4A, and $C_7F_{15}N$+4-phenolsulfonic sodium at 25 °C in water, and $C_7F_{15}N$+SC4A in normal saline solution; [$C_7F_{15}N$] = 0.15 mM, [SC4A] = 0.04 mM, [4-phenolsulfonic sodium] = 0.16 mM.

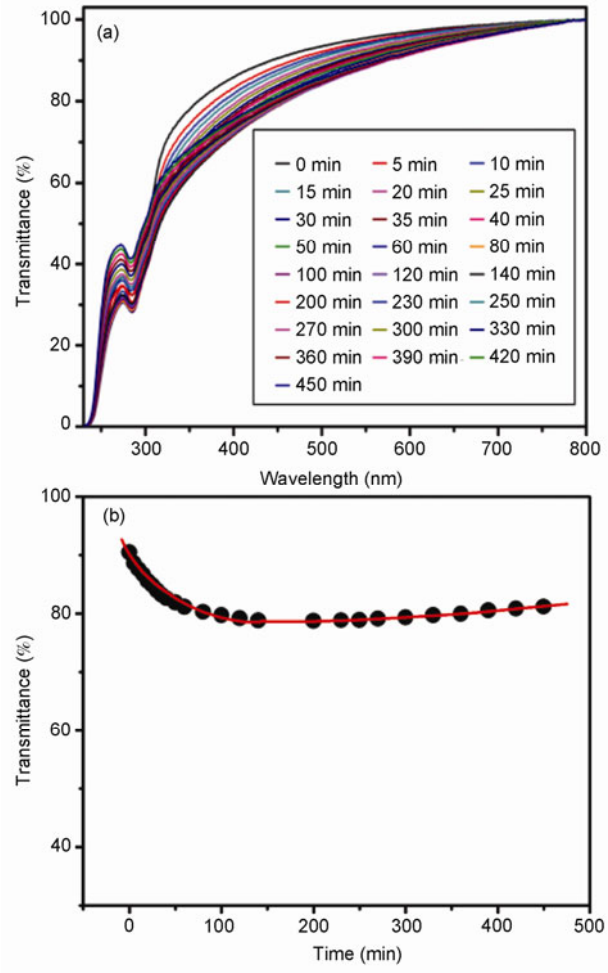

Figure 7 (a) Optical transmittance of the SC4A+$C_7F_{15}N$ (4:15) system on different time at 25 °C; (b) dependence of the transmittance at 450 nm on different time.

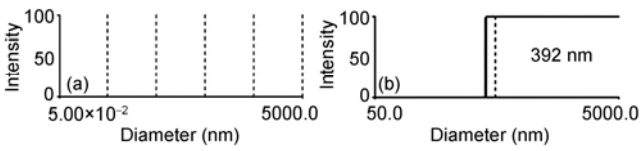

Figure 8 (a) DLS data of free $C_7F_{15}N$; (b) DLS data of the SC4A+$C_7F_{15}N$ aggregates.

displays a satisfactory sensitivity to the external temperature in Figure 10. The transmittance at 450 nm increases gradually when temperature ascends from 25 to 70 °C, and decreases inversely when temperature descends from 70 to 25 °C, reflecting the reversible disassembly/assembly. The left assembly curve is almost symmetric to the right disassembly one. High temperature disperses the aggregates, since heating weakens the enthalpy-driven complexation of sulfonatocalixarenes with organic guest molecules [45, 46]. SC4A, $C_7F_{15}N$, and 1:1 SC4A+$C_7F_{15}N$ simple complexes may be the final disassembled products [47].

We previously reported that SC4A formed the highly stable complex with MDBO, and the binding affinity is up to the magnitude of 10^7 M^{-1} [48]. It is reasonably envisaged to trigger the disassembly of the SC4A+$C_7F_{15}N$ aggregate by adding MDBO, representing a direct application of competitive binding. In Figure 11, the transmittance at 450 nm increases gradually upon continuous addition of MDBO, and reaches an equilibrium state when MDBO concentration is around 0.08 mM, which means that ca. 2 equiv of MDBO is required to fully disrupt the aggregates. The complexation-directed disruption presumably ascribes to expelling $C_7F_{15}N$ out of the cavity of SC4A by MDBO, since MDBO can be more tightly captured by SC4A than quaternary ammonium.

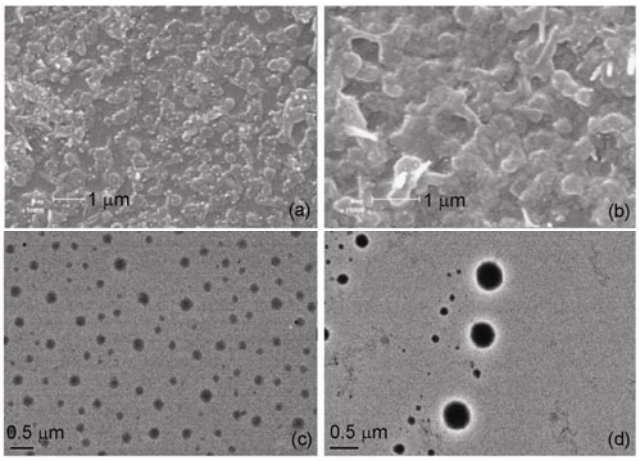

Figure 9 SEM (a and b) and TEM (c and d) images of the SC4A+$C_7F_{15}N$ aggregates.

4 Conclusions

We have successfully fabricated a self-assembled binary

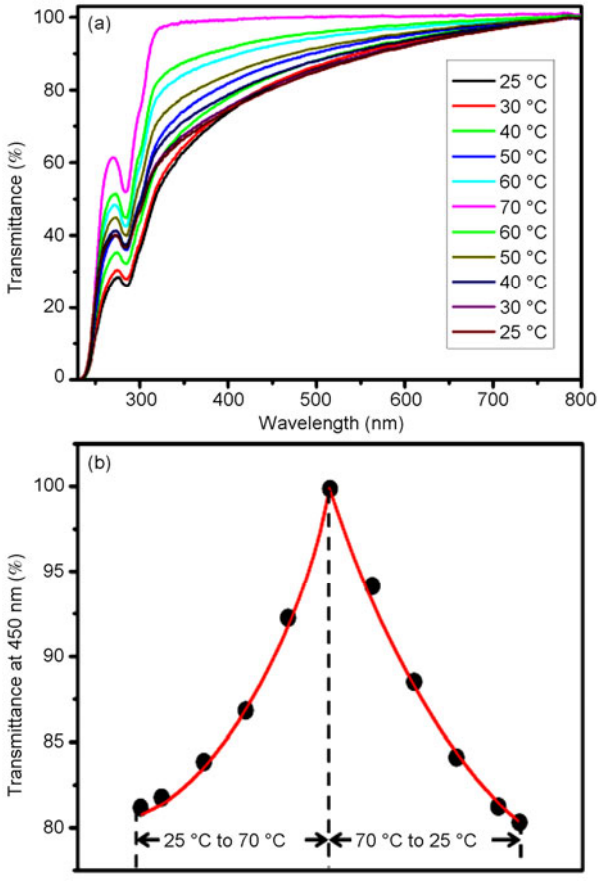

Figure 10 (a) Optical transmittance of the SC4A+$C_7F_{15}N$ aggregate at different temperatures (25–70 °C); (b) dependence of the transmittance at 450 nm on temperature between 25 and 70 °C.

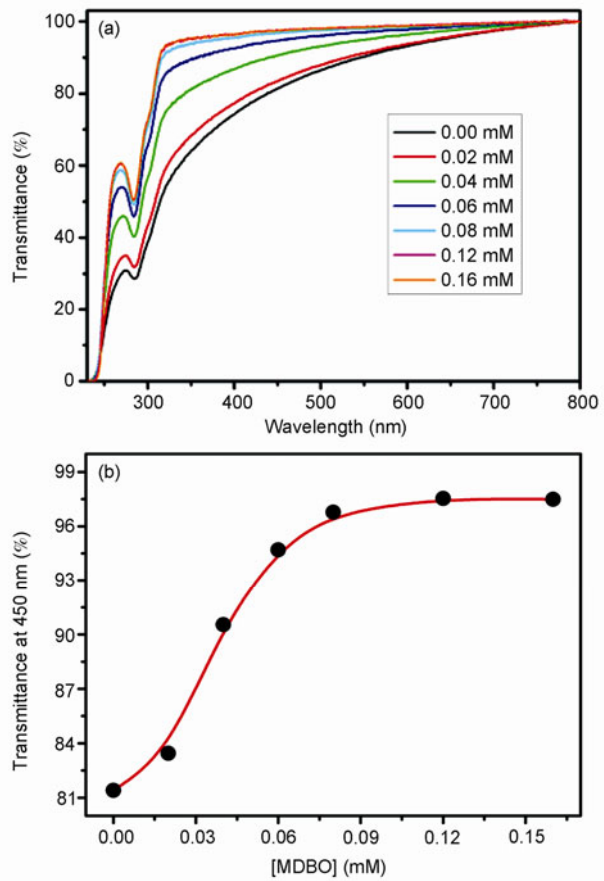

Figure 11 (a) Optical transmittance of the SC4A+$C_7F_{15}N$ aggregate at different concentrations of competitor MDBO; (b) dependence of the transmittance at 450 nm on concentration of competitor MDBO.

amphiphilic aggregate in virtue of the host-guest complexation of SC4A with fluorocarbon surfactant $C_7F_{15}N$. With the complexation of SC4A, the CAC value of $C_7F_{15}N$ decreases pronouncedly by a factor of ca. 100. Furthermore, the amphiphilic aggregate exhibits highly efficient responsiveness to external stimuli. High temperature and inclusion of competitor guest can lead to the disruption of the formed aggregate completely. We believe that with the advantages of fluorocarbon surfactants and the reversible nature of host-guest noncovalent assembly, the obtained assembly possesses promising applications in drug delivery and controlled release systems.

This work was supported by the National Basic Research Program of China (2011CB932502) and the National Natural Science Foundation of China (91227107 and 21172119), which were gratefully acknowledged.

1 Zhou SQ, Burger C, Chu B, Sawamura M, Nagahama N, Toganoh M, Hackler UE, Isobe H, Nakamura E. Spherical bilayer vesicles of fullerene-based surfactants in water: A laser light scattering study. *Science*, 2001, 291: 1944–1947
2 Mueller A, O'Brien DF. Supramolecular materials via polymerization of mesophases of hydrated amphiphiles. *Chem Rev*, 2002, 102: 727–758
3 Discher DE, Eisenberg A. Polymer vesicles. *Science*, 2002, 297: 967–973
4 Vriezema DM, Aragonès MC, Elemans JAAW, Cornelissen JJLM, Rowan AE, Nolte RJM. Self-assembled nanoreactors. *Chem Rev*, 2005, 105: 1445–1489
5 Kunitake T. Synthetische doppelschichtmembranen: Molekül-design, selbstorganisation und anwendungen. *Angew Chem Int Ed*, 1992, 31: 709–726
6 Kolusheva S, Shahal T, Jelinek R. Cation-selective color sensors composed of ionophore-phospholipid-polydiacetylene mixed vesicles. *J Am Chem Soc*, 2000, 122: 776–780
7 Perret F, Lazar AN, Coleman AW. Biochemistry of the *para*-sulfonato-calix[*n*]arenes. *Chem Commun*, 2006: 2425–2438
8 Coleman AW, Jebors S, Cecillon S, Perret P, Garin D, Marti-Battle D, Moulin M. Toxicity and biodistribution of *para*-sulfonato-calix [4]arene in mice. *New J Chem*, 2008, 32: 780–782
9 Uzunova VD, Cullinane C, Brix K, Nau WM, Day AI. Toxicity of cucurbit[7]uril and cucurbit[8]uril: An exploratory *in vitro* and *in vivo* study. *Org Biomol Chem*, 2010, 8: 2037–2042
10 Stella VJ, Rajewski RA. Cyclodextrins: Their future in drug formulation and delivery. *Pharm Res*, 1997, 14: 556–567
11 Uekama K, Hirayama F, Irie T. Cyclodextrin drug carrier systems. *Chem Rev*, 1998, 98: 2045–2076
12 Guo DS, Chen K, Zhang HQ, Liu Y. Nano-supramolecular assemblies constructed from water-soluble bis(calix[5]arenes) with porphyrins and their photoinduced electron transfer properties. *Chem Asian J*, 2009, 4: 436–445
13 Wang Z, Guo DS, Zhang J, Liu Y. Electro-responsive binary hydrogels based on calixarene and viologens. *Acta Chim Sinica*, 2012, 70: 1709–1715
14 Ikeda A, Shinkai S. Novel cavity design using calix[n]arene skeletons: Toward molecular recognition and metal binding. *Chem Rev*, 1997, 97: 1713–1734
15 Basilio N, Francisco V, Garcia-Rio L. Aggregation of *p*-sulfonatocalixarene-based amphiphiles and supra-amphiphiles. *Int J Mol Sci*, 2013, 14: 3140-3157
16 Kellermann M, Bauer W, Hirsch A, Schade B, Ludwig K, Böttcher C. Die erste Beschreibung einer strukturdefinierten micelle. *Angew Chem*, 2004, 116: 3019–3022; *Angew Chem Int Ed*, 2004, 43: 2959–2962
17 Lee M, Lee SJ, Jiang LH. Stimuli-responsive supramolecular nanocapsules from amphiphilic calixarene assembly. *J Am Chem Soc*, 2004, 126: 12724–12725
18 Wang K, Guo DS, Wang X, Liu Y. Multistimuli responsive supramolecular vesicles based on the recognition of *p*-sulfonatocalixarene and its controllable release of doxorubicin. *ACS Nano*, 2011, 5: 2880–2894
19 Francisco V, Basilio N, Garcia-Rio L, Leis JR, Maques EF, Vázquez-Vázquez C. Novel catanionic vesicles from calixarene and single-chain surfactant. *Chem Commun*, 2010, (46): 6551–6553
20 Wang K, Guo DS, Liu Y. Temperature-controlled supramolecular vesicles modulated by *p*-sulfonatocalix[5]arene with pyrene. *Chem Eur J*, 2010, 16: 8006–8011
21 Li ZQ, Hu CX, Cheng YQ, Xu H, Cao XL, Song XW, Zhang HY, Liu Y. Supramolecular vesicles of cationic gemini surfactants modulated by *p*-sulfonatocalix[4]arene. *Sci China Chem*, 2012, 55: 2063–2068
22 Danylyuk O, Suwinska K. Solid-state interactions of calixarenes with biorelevant molecules. *Chem Commun*, 2009: 5799–5813
23 Guo DS, Wang K, Wang YX, Liu Y. Cholinesterase-responsive supramolecular vesicle. *J Am Chem Soc*, 2012, 134:10244–10250
24 Chécot F, Lecommandoux S, Gnanou Y, Klok HA. Water-soluble stimuli-responsive vesicles from peptide-based diblock copolymers. *Angew Chem Int Ed*, 2002, 41: 1339–1343
25 Johnsson M, Wagenaar A, Engberts JB. Sugar-based gemini surfactant with a vesicle-to-micelle transition at acidic pH and a reversible vesicle flocculation near neutral pH. *J Am Chem Soc*, 2003, 125: 757–760
26 Orihara Y, Matsumura A, Saito Y, Ogawa N, Saji T, Yamaguchi A, Sakai H, Abe M. Reversible release control of an oily substance using photoresponsive micelles. *Langmuir*, 2001, 17: 6072–6076
27 Mynar JL, Goodwin AP, Cohen JA, Ma Y, Fleming GR, Fréchet JMJ. Two-photon degradable supramolecular assemblies of linear-dendritic copolymers. *Chem Commun*, 2007: 2081–2082
28 Power-Billard KN, Spontak RJ, Manners I. Redox-active organometallic vesicles: Aqueous self-assembly of a diblock copolymer with a hydrophilic polyferrocenylsilane polyelectrolyte block. *Angew Chem Int Ed*, 2004, 43: 1260–1264
29 Szymczyk K, Jańczuk B. Surface tension of polytetrafluoroethylene and polymethyl methacrylate under the influence of the fluorocarbon surfactant film. *Ind Eng Chem Res*, 2012, 51: 14076–14083
30 Eastoe J, Rogers SE, Martin LJ, Paul A. Fluorosurfactants at structural extremes: Adsorption and aggregation. *Langmuir*, 2006, 22: 2034–2038
31 Kissa E. Fluorinated surfactants: Synthesis, properties, applications. In *Surfactant Science Series*. *Vol. 50*. Marcel Dekker: New York, 1994
32 Kissa E. Fluorinated surfactants and repellents, second ed. *Surfactant Science Series, Vol. 97*. Marcel Dekker: New York, 2001
33 Gutsche CD, Levine JA. Calixarenes. 6. Synthesis of a functionalizable calix[4]arene in a conformationally rigid cone conformation. *J Am Chem Soc*, 1982, 104: 2652–2653
34 Gutsche CD, Muthukrishnan R. Calixarenes. 1. Analysis of the product mixtures produced by the base-catalyzed condensation of formaldehyde with *para*-substituted phenols. *J Org Chem*, 1978, 43: 4905–4906
35 Lei YB, Hurst JK. Reduction potentials of vesicle-bound viologens. *J Phys Chem*, 1991, 95: 7918–7925
36 Musilek K, Komloova M, Zavadova V, Holas O, Hrabinova M, Pohanka M, Dohnal V, Nachon F, Dolezal M, Kuca K, Jung YS. Preparation and *in vitro* screening of symmetrical bispyridinium cholinesterase inhibitors bearing different connecting linkage—initial study for Myasthenia gravis implications. *Bioorg Med Chem Lett*, 2010, 20: 1763–1766

37 Kalyanasundaram K, Thomas JK. Environmental effects on vibronic band intensities in pyrene monomer fluorescence and their application in studies of micellar systems. *J Am Chem Soc*, 1977, 99: 2039–2044
38 Krieg M, Pileni MP, Braun AM, Gratzel M. Micelle formation and surface activity of functional redox relays: Viologens substituted by a long alkyl chain. *J Colloid Interface Sci*, 1981, 83: 209–213
39 Diaz A, Quintela PA, Schuette JM, Kaifer AE. Complexation of redox-active surfactants by cyclodextrins. *J Phys Chem*, 1988, 92: 3537–3542
40 Lee Y, Lee C. Electrochemical behavior of viologens with long alkyl chains depending on their concentrations and the concentration of micelles and cyclodextrins. *Bull Korean Chem Soc*, 1999, 20: 1–8
41 Rehm M, Frank M, Schatz J. Water-soluble calixarenes—self-aggregation and complexation of noncharged aromatic guests in buffered aqueous solution. *Tetrahedron Lett*, 2009, 50: 93–96
42 Guo X, Szoka FC. Chemical approaches to triggerable lipid vesicles for drug and gene delivery. *Acc Chem Res*, 2003, 36: 335–341
43 Drummond DC, Zignani M, Leroux J. Current status of pH-sensitive liposomes in drug delivery. *Prog Lipid Res*, 2000, 39: 409–460
44 Nakayama M, Okano T, Miyazaki T, Kohori F, Sakai K, Yokoyama M. Molecular design of biodegradable polymeric micelles for temperature-responsive drug release. *J Controlled Release*, 2006, 115 : 46–56
45 Wang K, Guo DS, Zhang HQ, Li D, Zheng XL, Liu Y. Highly effective binding of viologens by *p*-sulfonatocalixarenes for the treatment of viologen poisoning. *J Med Chem*, 2009, 52: 6402–6412
46 Guo DS, Wang K, Liu Y. Selective binding behaviors of *p*-sulfonatocalixarenes in aqueous solution. *J Inclusion Phenom Macrocyclic Chem*, 2008, 62: 1–21
47 Guo DS, Wang LH, Liu Y. Highly effective binding of methyl viologen dication and its radical cation by *p*-sulfonatocalix[4,5]arenes. *J Org Chem*, 2007, 72: 7775–7778
48 Zhao HX, Guo DS, Liu Y. Binding behaviors of *p*-sulfonatocalix[4]arene with gemini guests. *J Phys Chem B*, 2013, 117: 1978–1987